A Parametric Analysis of the Transient Forced Response of Noncontacting Coned-Face Gas Seals

Itzhak Green

George W. Woodruff School of Mechanical Engineering,
Georgia Institute of Technology,
Atlanta, GA 30332-0405
e-mail: itzhak.green@me.gatech.edu

Roger M. Barnsby

Pratt and Whitney,
United Technologies Corporation,
East Hartford, CT 06108

A properly designed mechanical face seal must satisfy two requirements: (1) the seal must be stable, and (2) the seal forced response must be such that the stator tracks the misaligned rotor with the smallest clearance possible, with the smallest relative tilt, and with the largest minimum film thickness. The stability issue was investigated in a previous paper. Here a numerical solution is presented for the transient response of a noncontacting gas lubricated face seal that is subjected to stator and rotor forcing misalignments. The seal dynamic response is obtained in axial and angular modes of motion in a coupled analysis where the Reynolds equation and the equations of motion are solved simultaneously. The steady-state response is first identified for a reference case. Subsequently a parametric study is performed to gauge the influence of the various seal effects, such as speeds, inner to outer radii ratios, face coning heights, pressure drops, support stiffness and damping, and forcing misalignments. The transient responses to static stator misalignment and rotor runout are given, showing that properly designed coned face seals can operate in a stable mode with the stator tracking dynamically a misaligned rotor. [DOI: 10.1115/1.1401015]

Introduction

Mechanical face seal modes of failure are mostly well defined, e.g., face wear, cracking, blistering, thermal and mechanical warping, excessive leakage, etc. A variety of reasons can cause such failure modes but often these are the result of poor dynamic behavior of the seal. The dynamic behavior has two very distinctive features: stability and the steady-state response. Generally, stability deals with the natural response of the system where all forcing functions have been removed. Mathematically, stability is the investigation of the homogeneous equations of motion, and if a closed form solution is possible, a characteristic equation is formed and conditions are imposed (e.g., Routh-Hurwitz determinants) to guarantee that the eigenvalues contain a diminishing effect upon the natural response. In other words, it is in the nature of a stable system to diminish any disturbance, and restore the system normal state of operation. Conversely, in an unstable system even the smallest excitation will eventually cause the system to undergo large dynamic excursions from its designed point. The paper by Green and Barnsby [11] deals precisely with this mode of failure. Nonetheless, just guaranteeing stable operation, albeit being a prerequisite for a good design, is yet insufficient. The seal must have a favorable behavior also when it is repeatedly being forced by the various misalignments present in a practical seal. The investigation of the steady-state response is, therefore, of utmost importance and it is the subject of this work.

After a seal has been guaranteed to have stabilizing characteristics, the design must also ensure that the flexibly mounted stator tracks a misaligned rotor with the smallest relative misalignment between them. This would minimize the leakage and maximize the minimum film thickness, which in turn would promote noncontacting operation. Noncontacting seals have been preferred by the industry because they minimize the consequences of face wear, cracking, excessive leakage, etc.

The work on the dynamics of face seals concerns mostly incompressible fluids (Etsion [1–3]). Leefe [4], and Shapiro and Colsher [5] used piecewise integration schemes to solve the lubrication and dynamics problem for specific applications of gas seals. Zirkelback and San Andres [6] obtained static stiffness and damping coefficients of a spiral groove gas seal limited to axial mode only. Subsequently Zirkelback [7] performed a parametric study of these coefficients. The only simultaneous solution for the coupled lubrication and dynamics problem under forced conditions is given by Miller and Green [8]. That work provides a numerical formulation for the transient response of a spiral groove gas seal in both axial and angular modes of motion. However, a parametric analysis for the steady-state response for gas seals is not yet available.

Whether the fluid film is compressible or not, the same parameters (see Green and Etsion [9]) are expected to govern the dynamics of gas seals as well:

1 *Shaft Rotational Speed*—on one hand higher speeds tend to enhance the hydrodynamic effect, which generates an aligning tendency between stator and rotor (see Green and Etsion [10]). On the other hand, the inertia effect is strongly affected by speed, which may head off tracking between stator and rotor (see again same reference).

2 *Inner to Outer Radii Ratios*—the larger the sealing dam the better the sealing, because a larger sealing dam provides additional resistance to leakage. It is yet to be determined whether a larger sealing dam is also favorable from a dynamic point of view.

3 *Face Coning*—zero coning provides the smallest leakage. However, it has been already determined (Green and Barnsby [11]) that coning must form a converging gap in the direction of radial flow to provide positive hydrostatic fluid film stiffness. However, too much coning diminishes the stiffness effect and increases leakage. Zero coning, on the other hand, induces maximum damping capacity. Hence, a trade off must be made to determine how much coning is desired.

4 *Pressure Drop, and Inward Flow Versus Outward Flow*—if gas seals have similar trends to liquid seals then the higher the pressure drop the higher the film stiffness, and the better the stator

tracking of the misaligned rotor (Green and Etsion [9,10]). However, Green [12] has determined that outward flow of an inner pressurized seal has favorable stiffness compared to inward flow of an outer pressurized seal under identical conditions. This indeed has been confirmed in the stability analysis by Green and Barnsby [11].

5 *Support Stiffness and Damping*—Green and Barnsby [11] have shown that higher stiffness and damping increase the critical speed. However, higher stiffness and damping may impede the flexibly mounted stator from effectively tracking the misaligned rotor.

6 *Forcing Misalignments*—Intuitively, a larger rotor misalignment will induce a larger steady-state stator response. But in gas operation the film effects are nonlinear. It remains to be determined whether the stator response doubles when the rotor misalignment doubles. In addition, the stator itself may be misaligned prior to assembly because of tolerances or gravity. It is desirable to determine the relative importance between the two forcing misalignments, and establish the condition of synchronous tracking versus non-synchronous tracking.

Because of the nonlinear nature of the gas fluid film, the seal dynamic behavior is obtained numerically by integrating the time-dependent Reynolds equation simultaneously with the equations of motion. To minimize the tedious numerical work, the investigation conducted here adopts an approach by Green and Etsion [9] of a single perturbation technique, where a parameter is perturbed one at a time, and then it is reset after the solution is obtained. However, because a closed form solution is not available, the perturbation here is carried one level deeper, and more parameters are being investigated to increase the confidence in drawing meaningful conclusions. The solution technique here is similar to the work by Green and Barnsby [11]. However, the rotor and stator forcing misalignments add a significant change to the formulation of the problem. For completeness some definitions are repeated, but emphasis is given to the steady-state analysis.

Simultaneous Solution of Lubrication and Dynamics

The kinematics of a mechanical seal having a flexibly mounted stator configuration is shown in Fig. 1. The rotating seal seat (rotor) is rigidly mounted to the rotating shaft. The flexibly supported seal ring (stator) is attempting to track the misaligned rotor. The rotor misalignment is represented by a tilt γ_r measured between the out-normal to its plane and the axis of shaft rotation. Similarly, the stator may have prior to final attachment to the rotor, an initial misalignment, γ_{si}, measured with respect to the axis of shaft rotation. At rest, and with zero pressure differential, the stator is pressed against the rotor by supporting springs. This forces the stator into the same tilt as that of the rotor. During operation, however, the mating faces separate and the stator detaches from the rotor to assume its own tilt, γ_s. This tilt is a result of the combined effects of both γ_r and γ_{si}. The tilt angles γ_{si}, γ_r, and γ_s are all very small, typically less than one milliradian and, therefore, they can be treated as vectors. Since γ_{si} is fixed in space and γ_r is rotating at the shaft speed ω, the resultant vector γ_s will possess a time-varying precession (whirl) speed, $\dot{\psi}$. Green and Etsion [10], expressed the vector γ_s as follows:

$$\vec{\gamma}_s = \vec{\gamma}_{sl} + \vec{\gamma}_{sr}, \tag{1}$$

where $\vec{\gamma}_{sl}$ is the response to $\vec{\gamma}_{si}$ alone and it is fixed in space, while $\vec{\gamma}_{sr}$ is the response to $\vec{\gamma}_r$ alone and thus is whirling at the shaft speed. The relative misalignment between the stator and rotor, γ, is also a rotating vector, given by the vector subtraction and its magnitude

$$\vec{\gamma} = \vec{\gamma}_s - \vec{\gamma}_r; \quad |\gamma| = [\gamma_s^2 + \gamma_r^2 - 2\gamma_s\gamma_r\cos(\psi - \omega t)]^{1/2}. \tag{2}$$

Figure 2 shows the relative position between the seal components. The tilt vector γ_o is the relative misalignment γ in the special case when $\gamma_{sl} = 0$, so using Eqs. (1–2) gives
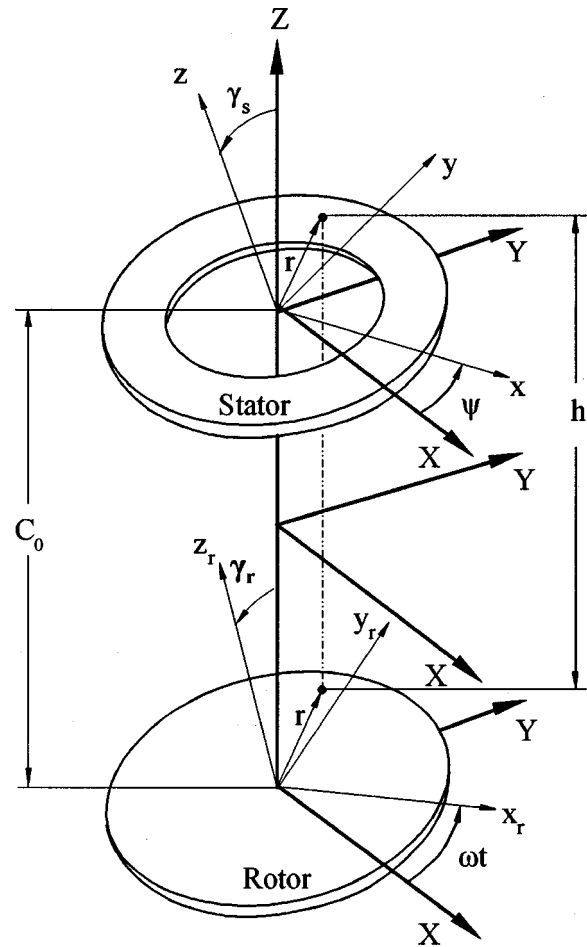
Fig. 1   Schematic of noncontacting mechanical face seal

$$\vec{\gamma}_o = \vec{\gamma}_{sr} - \vec{\gamma}_r. \tag{3}$$

The equations of motion of the flexibly mounted stator are (see Green and Etsion [9,10]):

$$I(\ddot{\gamma}_s - \dot{\psi}^2\gamma_s) = M_x \tag{4}$$

$$I(\ddot{\psi}\gamma_s + 2\dot{\psi}\dot{\gamma}_s) = M_y \tag{5}$$

$$m\ddot{Z} = F_Z, \tag{6}$$

where M_x and M_y are, respectively, the moments acting on the stator about axes x and y of a coordinate system xyz which whirls at a rate $\dot{\psi}$ within an inertial system XYZ (see Fig. 1). The tilt vector $\vec{\gamma}_s$ takes place about axis x of the rotating system, positioned by an angle ψ with respect to the inertial axis X. The moments M_x and M_y as well as the axial force F_z consist of contributions from both the flexible support and the fluid film. The support moments and force are

$$M_{sx} = K_s(\gamma_s\cos\psi - \gamma_s) - D_s\dot{\gamma}_s \tag{7}$$

$$M_{sy} = -K_s\gamma_{si}\sin\psi - D_s\dot{\psi}\gamma_s \tag{8}$$

$$F_{sZ} = -K_{sZ}Z - D_{sZ}\dot{Z}, \tag{9}$$

where K_{sZ} and D_{sZ} are, respectively, the axial stiffness and damping coefficients of the support. Note here that the term γ_{si} in Eqs. (7) and (8) is the initial stator misalignment that produces an inertial forcing function. This is the result of manufacturing and assembly imperfections (tolerances), or the action of gravity. Without loss of generality, it is arbitrarily assumed that γ_{si} coincides with the positive X direction.
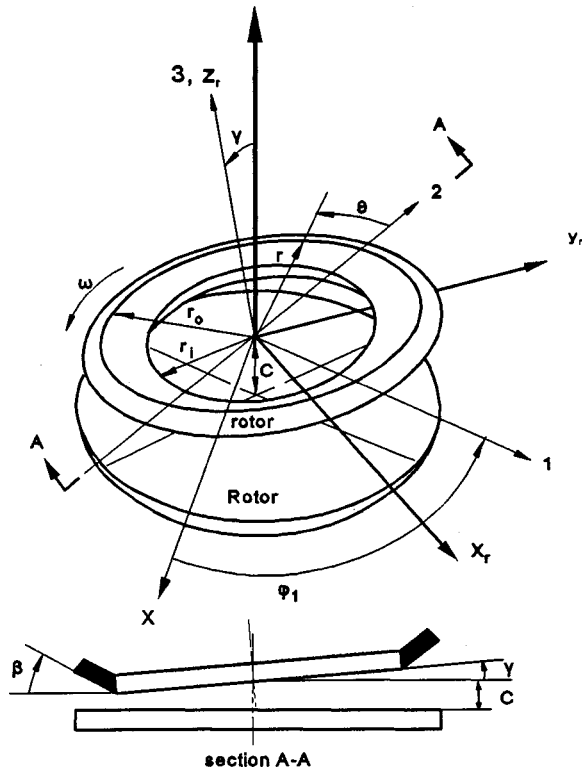
Fig. 2 Relative position between stator and rotor

The fluid film contribution to M_x, M_y, and F_Z is obtained by numerically integrating the pressure distribution in the sealing dam over the face area. The gas flow is assumed to be isothermal, isoviscous, and ideal; therefore, it is governed by the compressible form of the Reynolds equation (Gross [13])

$$\frac{\partial p}{\partial t} = \frac{1}{h}\left\{\vec{\nabla}\cdot\left[\frac{ph^3\vec{\nabla}p}{12\mu} - \frac{1}{2}\omega r p h \vec{i}_\theta\right] - p\frac{\partial h}{\partial t}\right\}, \quad (10)$$

where the operator $\vec{\nabla}$ is presumed here in cylindrical coordinates. This equation is subject to the boundary conditions (B.C.):

$$p(r_i,\theta,t) = p_i$$

$$p(r_o,\theta,t) = p_o$$

$$p(r,0,t) = p(r,2\pi,t),$$

and to the initial condition of pressure distribution within the sealing dam

$$p(r,\theta,0) = p_{IC}(r,\theta),$$

where $P_{IC}(r,\theta)$ is given by Green and Barnsby [11] assuming perfect alignment between stator and rotor at $t=0$. The local film thickness is expressed in an inertial frame, for the present analysis, however, the effect of rotor misalignment is added. Hence, using Figs. 1 and 2 leads to

$$h = C_o + Z + \beta(r - r_i) - \gamma_s r \sin(\psi - \theta) + \gamma_r r \sin(\omega t - \theta),\quad (11)$$

where C_o is the designed centerline clearance, β is the face coning, and γ_r is the rotor misalignment. The stator degrees of freedom are the axial displacement, Z, the nutation, γ_s, and the precession, ψ. At every instant of time the fluid film moments and force M_{fx}, M_{fy}, and F_{fZ} are obtained by numerically integrating the pressure over the sealing dam area

$$M_{fx} = \int_0^{2\pi}\int_{r_i}^{r_o} pr^2\sin(\theta - \psi)drd\theta \quad (12)$$

$$M_{fy} = -\int_0^{2\pi}\int_{r_i}^{r_o} pr^2\cos(\theta - \psi)drd\theta \quad (13)$$

$$F_z = \int_0^{2\pi}\int_{r_i}^{r_o} prdrd\theta. \quad (14)$$

Since and Z, γ_s, and ψ are time dependent then h, p, M_{fx}, M_{fy}, and F_Z are time dependent as well. The equations of motion (4)–(6) are recast now in a state space form including the support and fluid film effects,

$$\frac{\partial}{\partial t}\begin{Bmatrix} \dot{Z} \\ Z \\ \dot{\gamma}_s \\ \gamma_s \\ \dot{\psi} \\ \psi \end{Bmatrix} = \begin{Bmatrix} (F_{sZ}+F_{fZ})/m \\ \dot{Z} \\ (M_{sx}+M_{fx})/I + \dot{\psi}^2\gamma_s \\ \dot{\gamma}_s \\ [(M_{sy}+M_{fy})/I - 2\dot{\psi}\dot{\gamma}_s]/\gamma_s \\ \dot{\psi} \end{Bmatrix} \quad (15)$$

subject to the initial conditions $Z(0)$, $\dot{Z}(0)$, $\gamma_s(0)$, $\dot{\gamma}_s(0)$, $\psi(0)$, $\dot{\psi}(0)$. In the present analysis the seal is set into motion having synchronous whirl and parallel faces.

Note that the lubrication problem (Eq. (10)) and the dynamics problem (Eq. (15)) are coupled by the film thickness Eq. (11). Therefore, they must be solved simultaneously. Hence, a large state vector $\{\varphi\}$ is formed having the dimension of $ND+6$, where ND is the number of interior pressure nodes in the sealing dam, governed by Eq. (10). Conveniently these nodes are allocated first in the vector $\{\varphi\}$. The last six storage elements are reserved for the degrees of freedom given in state form in Eq. (15). This forms an explicit general system of equations

$$\frac{\partial}{\partial t}\{\varphi\} = \{RHS\}, \quad (16)$$

where $\{RHS\}$ is a column vector containing the right-hand-side of the relevant equation, i.e., either Eq. (10) or Eq. (15). This set of $ND+6$ equations is integrated in time by efficient multistep ordinary differential equation solvers (Shampine, [14]). The solution of Eq. (16) gives a simultaneous dynamic simulation for the transient pressure as well as the kinematical variables, yielding the seal motion.

Parametric Investigation

A typical reference case is selected (see Table 1). The analysis by Green and Barnsby [11] affirms that the reference case is stable. The same radial and circumferential discretization of $nr = 11$, and $nth = 313$ is used here as well. Hence $ND = (nr-2)*nth = 2817$, resulting in *2823* equations that are simultaneously being integrated in time. The forcing misalignments for the reference case are $\gamma_{si} = \gamma_r = 0.15\ mrad$. A single perturbation technique is adopted. First the motion for the reference case is solved. Then six parameters are perturbed each one at a time (with two exceptions that will be discussed later), the motion is obtained, and then each parameter is reset. Each of the six parameters is perturbed four times. This gives a total of 24 cases that are referenced by ij, where i refers to the cluster number, and j refers to the variation within the cluster. Each case is solved and the solutions are plotted side-by-side within their cluster to allow visual inspection and comparison between the responses. In each of the six figures (Figs. 3–8), the nondimensional values of the relative misalignment, $\gamma\cdot r_o/C_o$ (Eq. (2)), and the minimum film thickness, h_{min}/C_o (Eq. (11)), are plotted as a function of shaft revolution. (The axial displacement, Z/C_o, behaves throughout very similarly to $\gamma\cdot r_o/C_o$, and is therefore not plotted. It is taken into account, though, when h_{min}/C_o is calculated.) The case num-

Table 1   Seal runs

Parameter to vary	#	Λ	#	r_i/r_o (r_o=0.06m)	#	δ_h/C_o (C_o=6μm)	#	p_i, p_o	#	K_s, D_s	#	γ_{si}, γ_r
Base Case ω=20,000 rpm (ω=2094.4 rad/s) μ=1.8 (10)$^{-5}$ Pa·s C_o=6 μm p_i = 1 (10)^5 Pa p_o = 2 (10)^5 Pa r_i = 0.048 m r_o= 0.06 m Λ = 226.2 δ_h = 3 μm δ_h/C_o = 0.5 m= 1 kg I= 0.0018 kg·m^2 K_s= 5 (10)^5 N/m D_s= 300 N s/m γ_{si} =γ_r =0.15 mrad	11	ω=12,000 rpm ω=1256.6 rad/s Λ=135.7	21	$r_i/r_o \approx 0.7$ r_i = 0.042 m	31	δ_h/C_o = 0 δ_h = 0	41	p_i = 1 (10)^5 Pa p_o = 5 (10)^5 Pa	51	K_s=0 D_s=0	61	γ_{si} =0 γ_r =0.15 mrad
	12	ω=16,000 rpm ω=1675.5 rad/s Λ=181.0	22	r_i/r_o = 0.75 r_i = 0.045 m	32	δ_h/C_o =1 δ_h = 6 μm	42	p_i = 1 (10)^5 Pa p_o = 10 (10)^5 Pa	52	K_s= 5 (10)^5 N/m D_s=0	62	γ_{si} =0.15 mrad γ_r =0
	13	ω=24,000 rpm ω=2513.3 rad/s Λ=271.4	23	r_i/r_o = 0.85 r_i = 0.051 m	33	δ_h/C_o = 2 δ_h = 12 μm	43	p_i = 5 (10)^5 Pa p_o = 1 (10)^5 Pa δ_h = -3 μm	53	K_s=5 (10)^5 N/m D_s= 600 N s/m	63	γ_{si} =0.3 mrad γ_r =0.15 mrad
	14	ω=28,000 rpm ω=2932.2 rad/s Λ=316.7	24	r_i/r_o = 0.9 r_i = 0.054 m	34	δ_h/C_o = 3 δ_h = 18 μm	44	p_i = 10 (10)^5 Pa p_o = 1 (10)^5 Pa δ_h = -3 μm	54	K_s=9 (10)^5 N/m D_s= 300 N s/m	64	γ_{si} =0.15 mrad γ_r =0.3 mrad

ber is given in the figure legend along with the reference case. In each case the simulation continues until two successive revolutions reveal identical behavior (i.e., the two revolutions have a relative misalignment response of identical frequency, and the peak-to-peak and average values are less than a numerical tolerance of 10^{-4}). This is considered steady-state, and the simulation terminates. Thus, the transient plots provide the number of revolutions necessary to render steady-state. For example, only 14
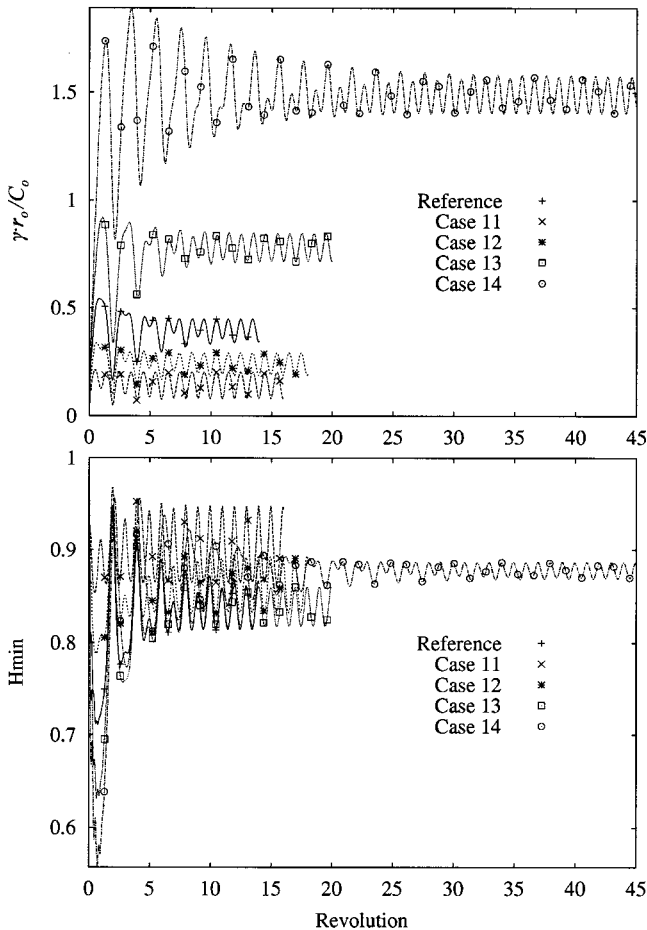

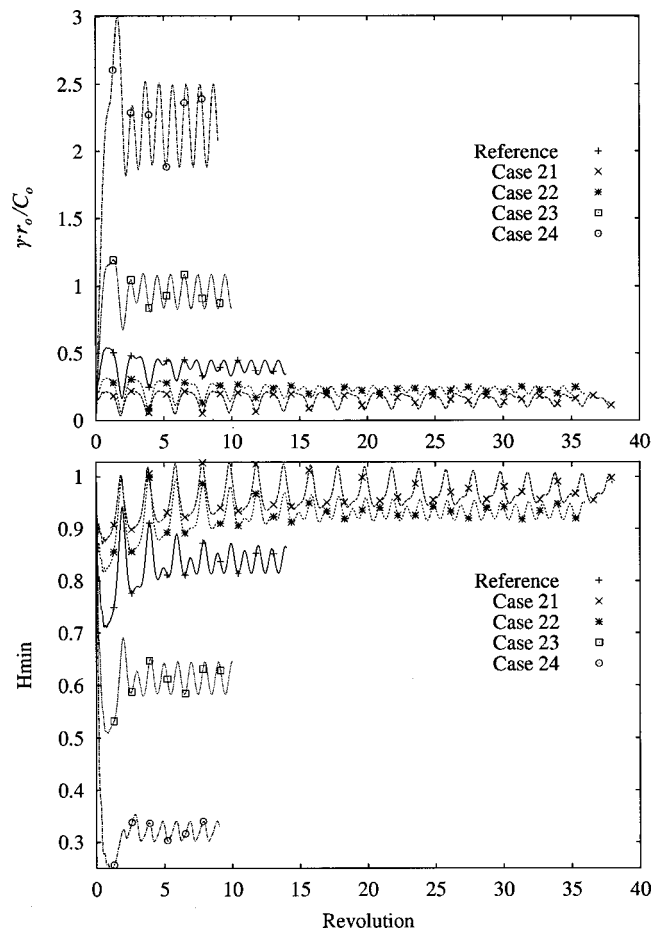**Fig. 3   Speed effects upon steady-state response**

Fig. 4   Radius ratio effects upon steady-state response
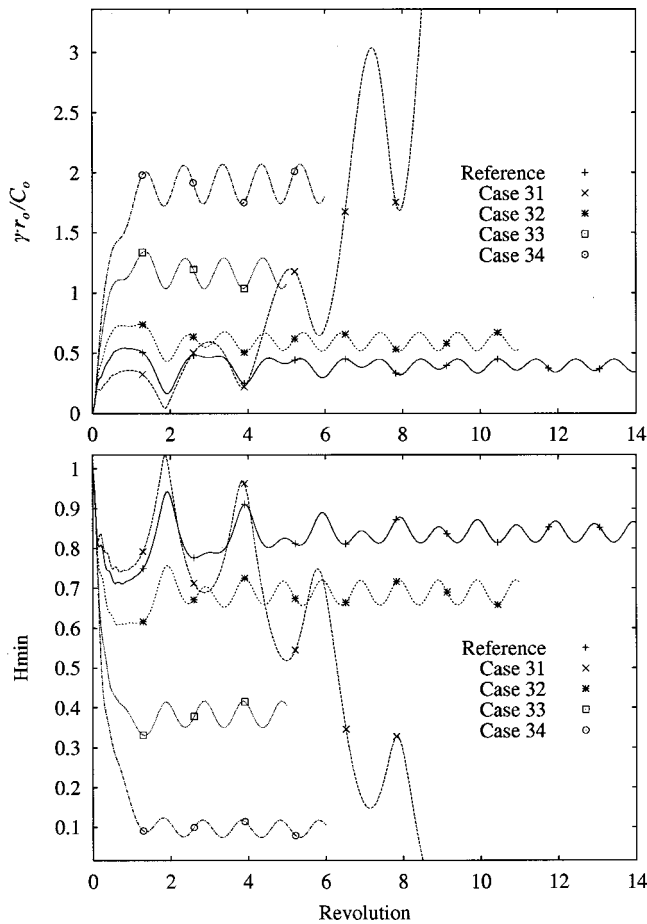
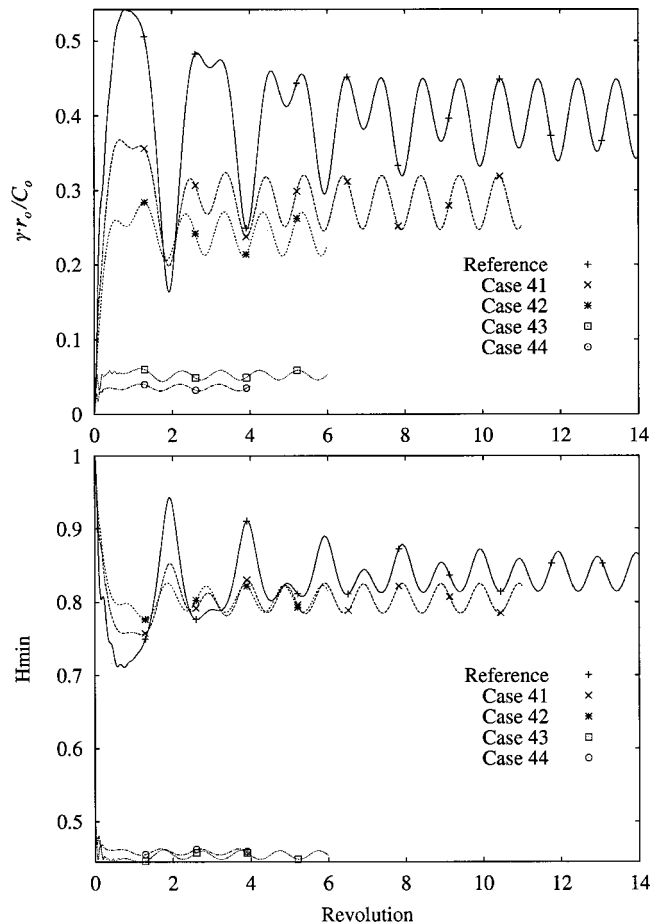**Fig. 5 Coning height effects upon steady-state response**

Fig. 6 Pressure drop effects upon steady-state response

revolutions are needed for the reference case, where 45 revolutions are needed for case 14. Respectively, the execution time is 9 min and 90 min on a 550 MHz PC.

An ideal seal should have Z/C_o and $\gamma \cdot r_o/C_o$ approach zero, while h_{min}/C_o approaches unity. These values minimize the flow rate and likelihood of contact. Thus, the larger the deviation from these values the worse is the seal. The mass flow rate, averaged over one revolution before steady state, for all cases is given in Table 2, where positive values indicate radial outward flow. It should be emphasized that the analysis that follows is restricted to the reference case and to the perturbations performed. Extrapolation to other cases should be made judiciously because of the highly nonlinear nature of the problem.

Speed Effect. From Fig. 3 it can be seen that the relative misalignment behaves nonlinearly with speed. The inertia-speed effects force the faces to open up and be more misaligned, thus causing the leakage to increase dramatically (e.g., the flow in case 14 is greater by a factor of 6.42 compared to the reference case). An initial half-frequency transient can be seen, particularly at the higher speeds, which is consistent with the transient analysis by Green and Barnsby [11]. But since all these cluster cases are stable, the transients diminish in time.

Radius Ratio. From Fig. 4 it is obvious that the smallest ratio of 0.7 has the best (smallest) steady-state response, being almost unaffected by the forcing misalignments. Conversely, the largest ratio of 0.9 has the worst response running at a dangerously small minimum film thickness. It is concluded that the smaller the radius ratio the higher fluid film stiffness and damping properties. Also, the calculated leakage is 53 times larger at the radius ratio of

0.9 than that of 0.7. Here, the largest sealing dam proves to be the best in terms of minimal steady-state response and leakage.

Coning Height. It is evident from Fig. 5 that the coning of the reference case is the best among these cluster cases, yielding the smallest steady-state response and the largest minimum film thickness. Looking at the two extremes of zero coning (case 31) and the largest coning (case 34), both have poor dynamic responses. Particularly the zero coning case becomes dynamically unstable that ends in face contact in about eight revolutions. This unstable behavior is consistent with the finding by Green and Barnsby [11]. Hence, it is concluded that there is an optimal coning, which seems to be close to the reference value. The reference case also has the smallest leakage of all these cluster cases and, as expected, the larger the coning the larger the leakage.

Pressure Drop. The magnitude of the pressure drop and its direction can have dramatic effects upon the dynamics of face seals. From observing the responses in Fig. 6 it is concluded that the reference case (having the smallest pressure drop) has the largest (worst) steady-state response amongst these cluster cases. The higher the pressure drop the smaller the response. The reference case and cases 41, and 42 represent inward radial flow. The flow rate (leakage) is proportional to $|P_o^2 - P_i^2|$ when the faces are perfectly aligned, and would obviously increase with the relative misalignment and the axial displacement. However, because the steady-state response is smaller at higher pressure drops it mitigates the leakage effect compared to lower pressure drop cases. For example, the leakage in case 42 is only 22.1 times larger than the reference case when theoretically a factor of 33 would be expected.
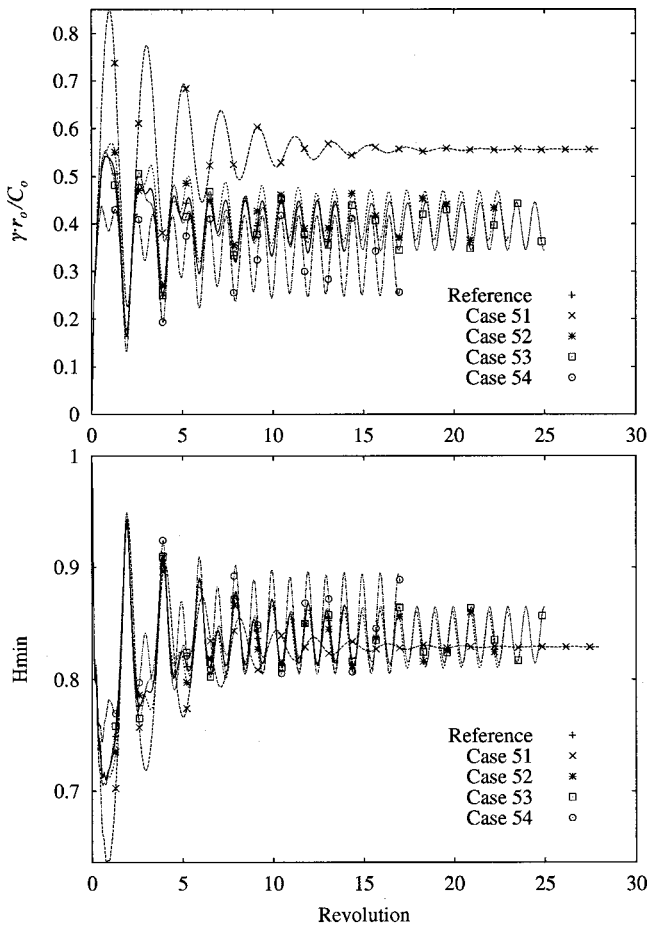
Fig. 7 Support stiffness and damping effects upon steady-state response

Fig. 8 Forcing misalignments effects upon steady-state response

The best steady-state performances in this cluster are obtained in cases 43 and 44, in which the pressure drop is reversed to impose outward flow seals. To comply with stability requirements (Green and Barnsby [11]) also the coning has to be reversed to form a converging gap in the radial direction of flow. The magnitude of coning height δ_h, though, is retained at reference value. It is evident that outward flow seals (inside pressurized) are far superior to the inward flow seals (outside pressurized). Cases 43 and 44 have average steady-state relative misalignments in the order of *0.052* and *0.036*, respectively, compared to *0.25–0.40* of the other cases in this cluster that represent inward flow. The peak-to-peak values are also an order of magnitude smaller in cases 43 and 44, where additionally their nondimensional axial displacements, Z/C_o, are both less than *0.01*. Such very small relative responses approach the ideal value of zero indicating almost perfect tracking between stator and rotor. The minimum film thicknesses in cases 43 and 44 are smaller because negative tapering creates OD film thicknesses smaller than ID film thicknesses, but the almost perfect dynamic response compensates for that. Also, the transients diminish rapidly and steady-state is achieved in six revolutions in case 43 and in four revolutions in case 44. This superior dynamic behavior is attributed to elevated fluid film stiffness (see Green [12]).

Moreover, the flow rates (see Table 2) in cases 43 and 44 are about an order of magnitude smaller than cases 41 and 42, respectively. Hence, not only that outward flowing seals are superior to inward flowing seals in their transient responses and stability (Green and Barnsby [11]), their sealing capability and steady-state responses are also superior.
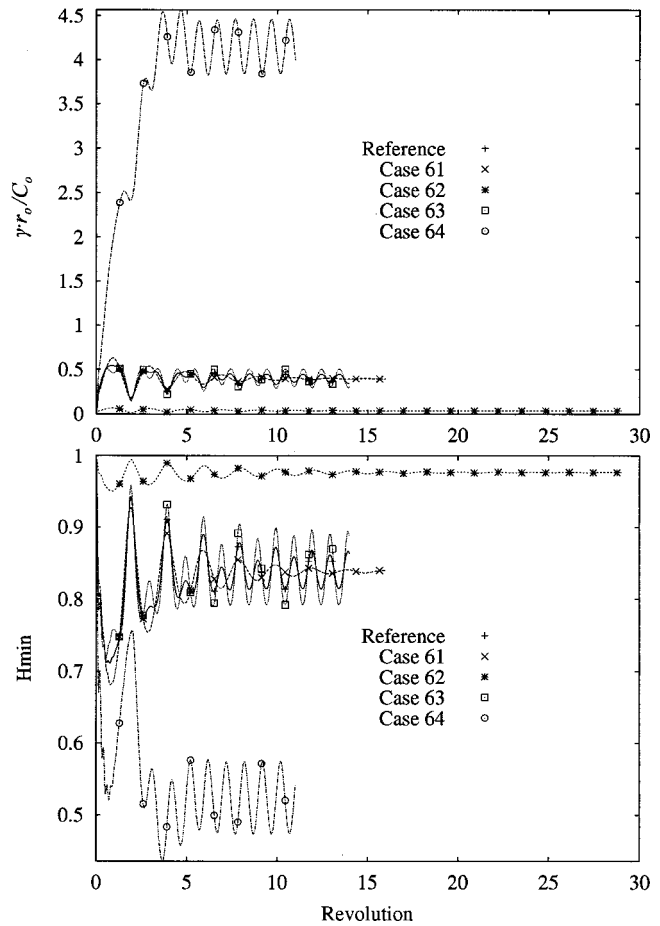
Support Stiffness and Damping. The first of two cases of synchronous tracking occurs when the stiffness and damping of the support vanish (case 51). In which case the forcing function caused by the initial stator misalignment is immaterial (see Eqs. (7–8)), causing the stator to synchronously track the misaligned rotor at steady-state. However, case 51 has the largest response in magnitude in this cluster, and it is not the most favorable case. Not many differences in the responses are recorded between the reference case and cases 52 and 53, indicating that the sensitivity to support damping is practically insignificant at these values. The best case 54 shows that increasing the support stiffness decreases the steady-state responses and thus has a more profound effect than damping. The general trend is that at these stated values the higher the support stiffness and damping the better the responses.

Table 2   Mass flow rates, kg/s

Parameter varied	#	Λ	#	r_i/r_o (r_o=0.06m)	#	δ_h/C_0 (C_0=6μm)	#	P_i, P_o	#	K_s, D_s	#	γ_{si}, γ_r
Assumed gas density at ambient conditions, ρ=1.0 kg/m³	11	-7.939E-06	21	-5.649E-06	31	unstable	41	-6.939E-05	51	-1.621E-05	61	-1.183E-05
	12	-8.912E-06	22	-7.597E-06	32	-1.841E-05	42	-2.633E-04	52	-1.232E-05	62	-7.579E-06
Base Case, kg/s	13	-2.516E-05	23	-3.746E-05	33	-4.801E-05	43	1.238E-05	53	-1.187E-05	63	-1.217E-05
-1.191E-05	14	-7.642E-05	24	-2.989E-04	34	-1.258E-04	44	4.909E-05	54	-1.064E-05	64	-7.492E-04

But this has to be carefully examined at values that deviate largely from the reference case, because extremely large support stiffnesses may impede tracking.

Forcing Misalignments. The second case of synchronous tracking occurs when the initial stator misalignment vanishes (case 61), in which the stator has to track only one forcing function which is the rotor runout (misalignment). The best case 62 represents a perfectly aligned rotor, and thus the stator steady-state response is static, where the pressure differential overwhelms the initial stator misalignment to form almost a perfectly aligned seal at its designed clearance. Obviously, the most effort in seal design should be devoted to minimize the imperfections and thus the forcing misalignments. This, however, is easier said than done, because practical system would always possess misalignments caused by manufacturing and assembly imperfections, misalignment of flexible shafts, gravity, machine deterioration, etc. It is reassuring, however, that the simulation reaffirms intuitive expectations. What is not intuitive is the fact that doubling the rotor runout alone, launches the system into a dynamic response that is about an order of magnitude larger in both, the relative misalignment and the axial displacement. This has detrimental effects on the minimum film thickness and leakage, which in case 64 is larger by a factor of 62.9 than the reference case. Case 64, when compared to the reference case, clearly demonstrates the strong nonlinear dynamic behavior of the system.

Conclusions

The steady-state response of a gas lubricated face seal having a flexibly mounted stator configuration has been analyzed by simultaneously solving the Reynolds equation and the equations of motion, which include forcing misalignments. A single perturbation investigation about a reference case has revealed the influence of the various parameters that govern seals dynamic behavior. With the exception of only one transient response (case 31) the reference and perturbed cases exhibited stable responses. It has been found that the steady-state responses have very different sensitivities to the parameters and thus result in very different transient responses. The single perturbation technique is not most comprehensive because it would be difficult to predict what might happen when two or more parameters are perturbed at the same time. However, some trends have surfaced which may still be useful in the design of gas face seal having a floating stator type. Lower speeds, larger sealing dams, optimal coning, larger pressure drops, and smaller forcing misalignments, would generally contribute to smaller dynamic responses. The leakage has to be examined on a case by case basis, but generally a smaller dynamic response (not attributed to a higher pressure drop) results in a smaller leakage. Support effects in pressurized gas seals would typically influence very little the steady-state responses. Inside pressurized seals have been proven again to have superior dynamic responses compared to outside pressurized seals.

Nomenclature

C = centerline clearance
C_o = design clearance
D_Z = axial damping coefficient
D = angular damping coefficient
F = force
h = local film thickness
I = transverse moment of inertia
K_Z = axial stiffness coefficient
K = angular stiffness coefficient
M = moment
M_{Xi} = moment due to stator initial misalignment
m = stator mass
p = pressure
r = radial coordinate
t = time
Z = axial degree of freedom
β = face coning angle
γ = relative misalignment
γ_o = relative misalignment caused by rotor runout alone
γ_r = rotor runout
γ_s = stator nutation
γ_{si} = stator initial misalignment
γ_{sl} = steady-state stator response due to γ_{si} alone
γ_{sr} = steady-state stator response due to γ_r alone
δ_h = coning height, $\beta(r_o - r_i)$
θ = angular coordinate
Λ = compressibility number, $6\mu\omega r_o^2/p_a C_o^2$
μ = viscosity
ψ = precession
ω = shaft angular velocity

Subscripts

a = ambient
f = fluid film
i = inner radius
o = outer radius
r = rotor
ref = reference case
s = stator, or flexible support

References

[1] Etsion, I., 1982, "A Review of Mechanical Face Seal Dynamic," Shock Vib. Dig., **14**, No. 3, pp. 9–14.
[2] Etsion, I., 1985, "Mechanical Face Seal Dynamics Update," Shock Vib. Dig., **17**, No. 4, pp. 11–16.
[3] Etsion, I., 1991, "Mechanical Face Seal Dynamics 1985–1989," Shock Vib. Dig., **23**, No. 4, pp. 3–7.
[4] Leefe, S., 1994, "Modeling of Plain Face Gas Seal Dynamics," *14th International Conference on Fluid Sealing*, BHR Group Conference Series, No. 9, pp. 397–424.
[5] Shapiro, W., and Colsher, R., 1974, "Steady State and Dynamic Analysis of a Jet-Engine, Gas Lubricated Shaft Seal," ASLE Trans., **17**, No. 3, pp. 190–200.
[6] Zirkelback, N., and San Andrés, L., 1998, "Effect of Frequency Excitation on Force Coefficients of Spiral Groove Gas Seals," ASME J. Tribol., **121**, No. 4, pp. 853–863.
[7] Zirkelback, N., 2000, "Parametric study of Spiral Groove Gas Face Seals," STLE Tribol. Trans., **43**, No. 2, pp. 337–343.
[8] Miller, B., and Green, I., 2000, "Numerical Formulation for the Dynamic Analysis of Spiral-Grooved Gas Face Seals," ASME J. Tribol., **123**, No. 2, pp. 395–403.
[9] Green, I., and Etsion, I., 1986, "Nonlinear Dynamic Analysis of Noncontacting Coned-Face Mechanical Seals," ASLE Trans., **29**, No. 3, pp. 383–393.
[10] Green, I., and Etsion, I., 1985, "Stability Threshold and Steady-State Response of Noncontacing Coned-Face Seals," ASLE Trans., **28**, No. 4, pp. 449–460.
[11] Green, I., and Barnsby, R. M., 2000, "A Simultaneous Numerical Solution for the Lubrication and Dynamic Stability of Noncontacting Gas Face Seals," ASME J. Tribol., **123**, No. 2, pp. 388–394.
[12] Green, I., 1987, "The Rotor Dynamic Coefficients of Coned-Face Mechanical Seals With Inward or Outward Flow," ASME J. Tribol., **109**, No. 1, pp. 129–135.
[13] Gross, W. A., 1980, *Fluid Film Lubrication*, John Wiley, New York.
[14] Shampine, L. F., 1994, *Numerical Solution of Ordinary Differential Equations*, Chapman and Hall, New York.